SSLP114 - Semi-infinite plane crack

Summary

This test makes it possible to validate the calculation of an asymptotic field by method XFEM. It is a question of checking if modeling XFEM represents the analytical solution accurately, of the breaking process. This analytical field is the exact solution to the problem of opening in mode I of a plane crack.

The field is a square plate, cut until the medium by a horizontal crack. A loading is imposed on the 4 edges to ensure an opening in mode rigorously I, conforms to the analytical solution. One applies limiting conditions of standard “displacement” to the not fissured edges, and of type “forces” on the edge cut by the crack.

To validate this approach, 3 modelings are planned:

- Modeling a: one carries out a simple calculation starting from linear elements (TRIA3) for a horizontal crack
- Modeling b: one carries out a simple calculation starting from quadratic elements (TRIA6) for a horizontal crack
- Modeling C: one inclines the crack to change the reference frame of the analytical formulas. To preserve the opening in mode I, one inclines the fields (forced and displacement) imposed on the edges. On the one hand, one evaluates the incidence of the form of the field on the results, since in theory, the asymptotic equations do not depend on the geometry of the field in the reference frame of the crack. In addition, one evaluates the robustness of calculation with the degradation of conditioning.

One tests the stress intensity factors KI, KII. For the mode I, one will have to find $KII=0$ and $KI\neq 0$, KI corresponding to the proportionality factor forced on the fields solution (see paragraph [3]).

In the same way, one checks also the exactitude of the calculation of the field of displacement calculated on the field, compared to the analytical solution.

1 Problem of reference

1.1 Geometry

Modeling A:
The structure 2D is a unit square plate ($LX=1$, $LY=1$), comprising a crack “leading” to a half-length [Figure 1.1-1]. The crack is right, horizontal and length $a=0,5$. One arbitrarily directs the crack of the flat rim towards the center.

The edges of the fields are noted in trigonometrical direction:
- $LIG1$ indicate the lower edge.
- $LIG2$ indicate the flat rim.
- $LIG3$ indicate the higher edge.
- $LIG4$ indicate the left edge.

The 4 edges of the field are used to impose the limiting conditions. On the edges not cut by the crack ($LIG1$, $LIG2$, $LIG3$) one imposes limiting conditions of Dirichlet, using the analytical solution in displacement (see paragraph [3]).

Let us note that the flat rim ($LIG4$) crossed by the crack, generates a singularity with the intersection. One observes a jump of displacement corresponding to the opening of the crack [Figure 2.3-1]. It is difficult to control this edge in displacement, since it is necessary analytically to clarify the condition of jump on the upper lip and the lower lip of the crack on the elements of edge cut by the crack. One circumvents this difficulty by imposing conditions of Neumann on this edge.

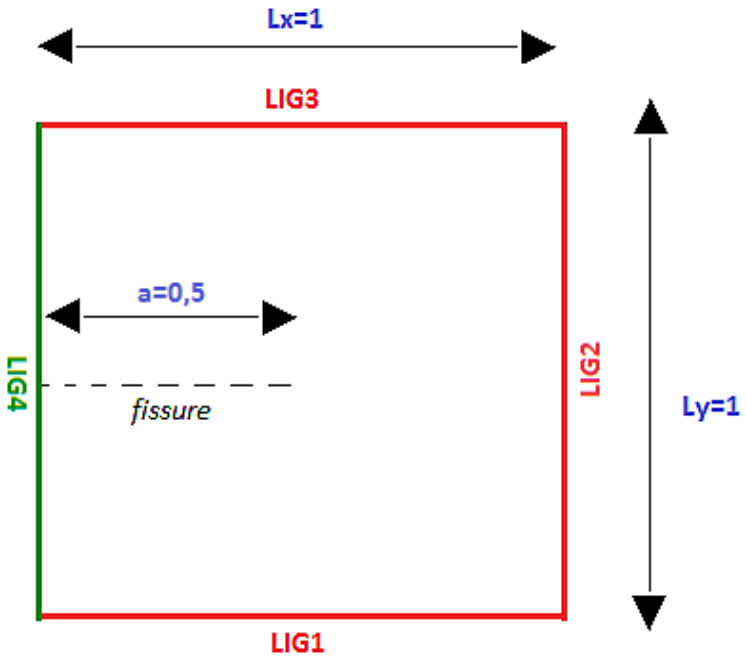

Figure 1.1-1: Geometry of the field

Modeling B:
Even geometry that modeling A.

Modeling C:

One inclines the crack of a variable angle such as $\alpha \epsilon \{0^\circ, 30^\circ, 60^\circ, 90^\circ, 120^\circ\}$ [Figure 1.1-2].

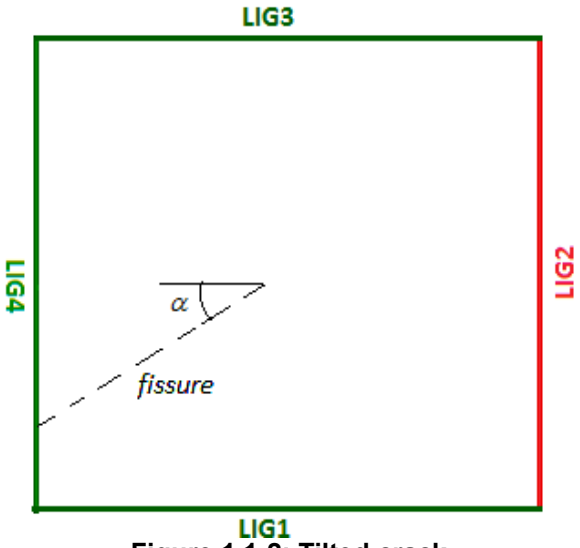

Figure 1.1-2: Tilted crack

Let us note that the crack lengthened. The new length is: $a = \frac{0,5}{max\left\{\left|\cos\left(\frac{\alpha \times \pi}{180}\right)\right|, \left|\sin\left(\frac{\alpha \times \pi}{180}\right)\right|\right\}}$.

1.2 Properties of material

Young modulus: $E = 10^5 Pa$
Poisson's ratio: $\nu = 0$

1.3 Boundary conditions and loadings

The loading is imposed thanks to mixed limiting conditions.

The not fissured edges are controlled in displacement, the fissured edge is controlled in force. In addition, the limiting conditions of Dirichlet (in displacement) fix the structure and prevent the appearance of rigid modes.

In modelings A and B, the crack cuts only the edge $LIG4$, One imposes a condition of Neumann on this edge and Dirichlet on the 3 other edges (see [Figure 1.3-1]).

In modeling C, one generalizes the preceding approach. For a slope higher than 45°, the crack cut is the lower edge ($LIG1$), that is to say the higher edge ($LIG3$). To these two edges also one applies a condition of Neumann. One thus imposes a condition of Dirichlet on the remaining edge ($LIG2$) to fix the rigid modes (see [Figure 1.3-2]). Limiting conditions being imposed symmetrically on the horizontal crack ($\alpha = 0$), calculations presented will be valid for $-135^\circ < \alpha < 135^\circ$

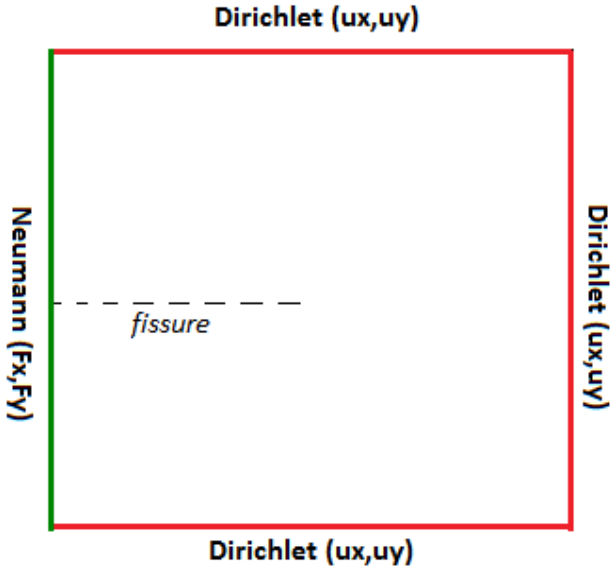

Figure 1.3-1: Mixed limiting conditions for modelings A and B

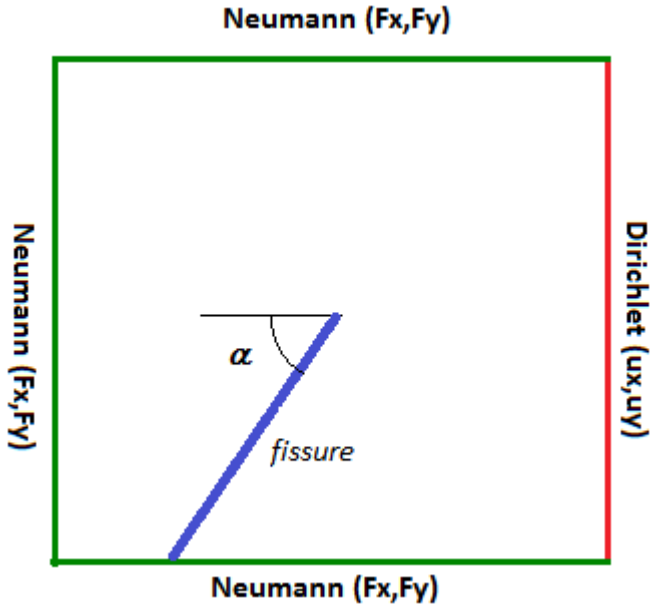

Figure 1.3-2: Mixed limiting conditions for modeling C

Imposed displacement corresponds to the exact analytical solution:

$$U_x=\frac{(1+\nu)}{E}\sqrt{\frac{r}{2\pi}}K_I\cos(\frac{\theta}{2})(3-4\nu-\cos\theta)$$

$$U_y=\frac{(1+\nu)}{E}\sqrt{\frac{r}{2\pi}}K_I\sin(\frac{\theta}{2})(3-4\nu-\cos\theta)$$

This solution depends on the polar coordinates related to the reference frame of the crack [Figure 1.3-3]. In the literature ([11]), the direction of the crack supports the axis $\vec{X}$. The axis $\vec{X}$ bottom of the

crack is directed towards outside. $\vec{Y}$ is orthogonal with $\vec{X}$, such as $(\vec{X},\vec{Y})$ form a direct reference mark.

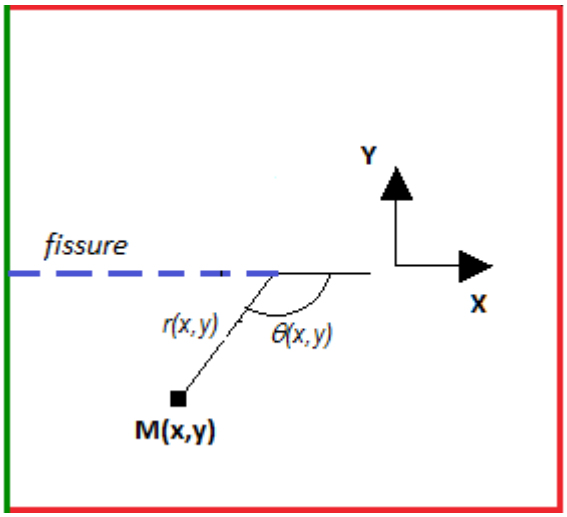

Figure 1.3-3: Local reference frame of the analytical formulas

Consequently, it is necessary to carry out a basic change to adapt the valid analytical equations in the reference frame of the crack, with a given reference mark. In particular, as the origin of the reference mark of the coordinates of the meshs is selected with the left lower corner of the field, one relocates the polar coordinates:

θ is the polar angle: $\theta(x,y)=arctan2(y-0.5,x-0.5)$

r the radial distance: $r(x,y)=\sqrt{(x-0.5)^2+(y-0.5)^2}$

The tensor of the constraints analytical solution is:

$$\sigma_{xx}=\frac{K_I}{\sqrt{2\pi r}}\cos\left(\frac{\theta}{2}\right)\left(1-\sin\left(\frac{\theta}{2}\right)\sin\left(\frac{3\theta}{2}\right)\right)$$

$$\sigma_{yy}=\frac{K_I}{\sqrt{2\pi r}}\cos\left(\frac{\theta}{2}\right)\left(1+\sin\left(\frac{\theta}{2}\right)\sin\left(\frac{3\theta}{2}\right)\right)$$

$$\sigma_{xy}=\frac{K_I}{\sqrt{2\pi r}}\sin\left(\frac{\theta}{2}\right)\cos\left(\frac{\theta}{2}\right)\cos\left(\frac{3\theta}{2}\right)$$

Then, one projects the tensor of the constraints to deduce the density of force from it to be applied to the flat rim ($LIG4$), of "outgoing" normal $-\vec{X}$.

The force to be applied is: $\vec{F}=\underline{\underline{\sigma}}.-\vec{X}$

It comes: $F_x=-\sigma_{xx}$ and $F_y=-\sigma_{xy}$

Modeling A:
Compared to the reference frame of the crack, the axes "aster" are directed in the same direction. Fields of displacement Ux and Uy of reference are applied to edges LIG1, LIG2, LIG3:

$$U_x=\frac{E}{2(1+\nu)}\sqrt{\frac{r}{2\pi}}K_I\cos(\frac{\theta}{2})(3-4\nu-\cos\theta)$$

$$U_y=\frac{E}{2(1+\nu)}\sqrt{\frac{r}{2\pi}}K_I\sin(\frac{\theta}{2})(3-4\nu-\cos\theta)$$

In the same way the tensor of constraints reference is preserved. One thus applies the same density of force clarified above to the edge $LIG4$.

$$F_x=-\sigma_{xx}\quad F_y=-\sigma_{xy}$$

Modeling B:
Same equations as modeling A.

Modeling C:
One inclines crack of an angle of $\alpha\in\{0^\circ,30^\circ,60^\circ,90^\circ,120^\circ\}$.

This rotation impacts it**polar angle**, it **field of displacement** and it **tensor of the constraints**. These sizes carry out a rotation of an angle α , compared to the reference mark code aster fixes.

$$\theta\rightarrow\theta-\alpha$$

However this transformation of the polar angle is not valid for all the angles, because the definition of the polar angle is not continuous. In the local reference frame, on both sides of the crack one observes an angular jump of 2π : lower lip with the upper lip one passes from $-\pi$ with π .

Consequently, the rotation of the crack must also propagate this angular discontinuity. All angles swept by the crack (grayed zone cf [Figure 1.3-4] and [Figure 1.3-5]) during rotation, undergo an angular jump of -2π or 2π ,

If $\alpha>0$ (the rotation of the crack is carried out downwards)
- In the zone $-\pi<\theta<-\pi+\alpha$ one a: $\theta\rightarrow\theta-\alpha+2\pi$
- In the zone $\pi>\theta>-\pi+\alpha$ one a: $\theta\rightarrow\theta-\alpha$

If $\alpha<0$ (the rotation of the crack is carried out upwards)
- In the zone $\pi>\theta>\pi+\alpha$ one a: $\theta\rightarrow\theta-\alpha-2\pi$
- In the zone $-\pi<\theta<\pi+\alpha$ one a: $\theta\rightarrow\theta-\alpha$

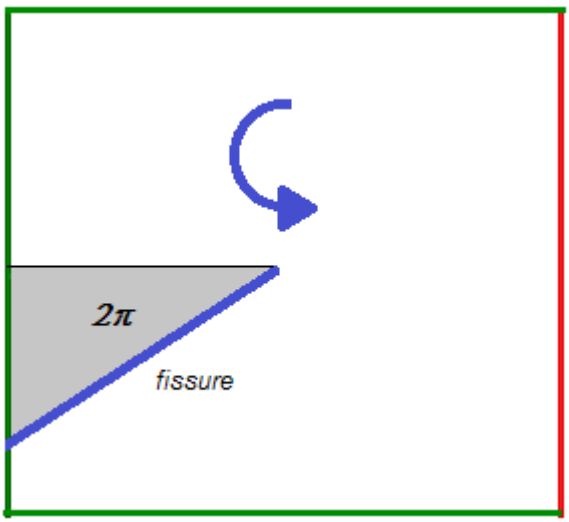

Figure 1.3-4: Angular field of jump (positive)

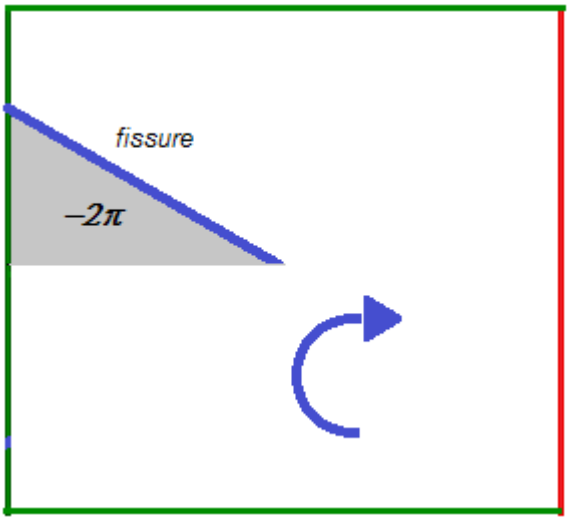

Figure 1.3-5: Angular field of jump (negative)

$\vec{U} \to R_\alpha \vec{U}$ where R_α is the matrix of rotation of angle α with $R_\alpha = \begin{bmatrix} \cos(\alpha) & -\sin(\alpha) \\ \sin(\alpha) & \cos(\alpha) \end{bmatrix}$

Consequently,

$$\vec{U} \to \begin{bmatrix} \cos(\alpha) U_x - \sin(\alpha) U_y \\ \sin(\alpha) U_x + \cos(\alpha) U_y \end{bmatrix}$$

The tensor of the deformations is also impacted by rotation:

$$\underline{\underline{\sigma}} \to R_\alpha \underline{\underline{\sigma}} R_{-\alpha}$$

$$\underline{\underline{\sigma}} \to \begin{bmatrix} \cos(\alpha) & -\sin(\alpha) \\ \sin(\alpha) & \cos(\alpha) \end{bmatrix} \begin{bmatrix} \sigma_{xx} & \sigma_{xy} \\ \sigma_{xy} & \sigma_{yy} \end{bmatrix} \begin{bmatrix} \cos(\alpha) & \sin(\alpha) \\ -\sin(\alpha) & \cos(\alpha) \end{bmatrix}$$

$$\underline{\underline{\sigma}} \to \begin{bmatrix} \cos(\alpha) & -\sin(\alpha) \\ \sin(\alpha) & \cos(\alpha) \end{bmatrix} \begin{bmatrix} \cos(\alpha)\sigma_{xx} - \sin(\alpha)\sigma_{xy} & \sin(\alpha)\sigma_{xx} + \cos(\alpha)\sigma_{xy} \\ \cos(\alpha)\sigma_{xy} - \sin(\alpha)\sigma_{yy} & \sin(\alpha)\sigma_{xy} + \cos(\alpha)\sigma_{yy} \end{bmatrix}$$

From where the final writing of the tensor of constraints:

$$\underline{\underline{\sigma}} \to \begin{bmatrix} \cos(\alpha)^2 \sigma_{xx} - \sin(2\alpha)\sigma_{xy} + \sin(\alpha)^2 \sigma_{yy} & -\frac{1}{2}\sin(2\alpha)(-\sigma_{xx} + \sigma_{yy}) + \cos(2\alpha)\sigma_{xy} \\ -\frac{1}{2}\sin(2\alpha)(-\sigma_{xx} + \sigma_{yy}) + \cos(2\alpha)\sigma_{xy} & \sin(\alpha)^2 \sigma_{xx} + \sin(2\alpha)\sigma_{xy} + \cos(\alpha)^2 \sigma_{yy} \end{bmatrix}$$

It is checked that rotation preserves the symmetry of the tensor and the trace, $tr(\underline{\underline{\sigma}}) = \sigma_{xx} + \sigma_{yy}$

In the programming of the command file, the horizontal crack is a typical case of tilted crack: all the equations depend on a slope α unspecified. To find modeling A and B, it is enough to make $\alpha = 0°$.

1.4 Reference solution

One imposes $K_I=1$.

In the reference frame related to the crack, the analytical equations become:

$$U_x=\frac{E}{2(1+\nu)}\sqrt{\frac{r}{2\pi}}\cos(\frac{\theta}{2})(3-4\nu-\cos\theta)$$

$$U_y=\frac{E}{2(1+\nu)}\sqrt{\frac{r}{2\pi}}\sin(\frac{\theta}{2})(3-4\nu-\cos\theta)$$

By linearity of the equations, the tensor of the constraints is affected by the same proportionality factor and becomes:

$$\sigma_{xx}=\frac{1}{\sqrt{2\pi r}}\cos\left(\frac{\theta}{2}\right)\left(1-\sin\left(\frac{\theta}{2}\right)\sin\left(\frac{3\theta}{2}\right)\right)$$

$$\sigma_{yy}=\frac{1}{\sqrt{2\pi r}}\cos\left(\frac{\theta}{2}\right)\left(1+\sin\left(\frac{\theta}{2}\right)\sin\left(\frac{3\theta}{2}\right)\right)$$

$$\sigma_{xy}=\frac{1}{\sqrt{2\pi r}}\sin\left(\frac{\theta}{2}\right)\cos\left(\frac{\theta}{2}\right)\cos\left(\frac{3\theta}{2}\right)$$

By construction, there does not exist mode II . In other words, one tests $K_{II}=0$.

Modeling A:

This modeling makes it possible to validate operator POST_ERREUR by comparing the computed values of the standard L^2 displacement and energy of the structure to the analytical values.

1.4.1 Calculation of the standard L² displacement

That is to say Ω the field occupied by the solid. The standard L^2 displacement is defined by :

$$\|\boldsymbol{u}\|_{L^2}^2=\int_\Omega\|\boldsymbol{u}\|^2\,dS\,.$$

One a:

$$\|\boldsymbol{u}\|^2=\left(\frac{1+\nu}{E}\right)^2\frac{r}{2\pi}K_I^2(\kappa-\cos\theta)^2\,,$$

for any point of Ω . One thus has:

$$\|\boldsymbol{u}\|_{L^2}^2=\left(\frac{1+\nu}{E}\right)^2\frac{K_I^2}{2\pi}\int_\Omega r(\kappa-\cos\theta)^2\,dS\,.$$

The field Ω is represented in Cartesian coordinates by $\Omega=[-a\,,a]\times[-a\,,a]$, where $a=LX/2=LY/2=1/2$, and perhaps represented in polar coordinates by:

$$\Omega=\left\{(r,\theta)\in\mathbb{R}\times\left[\frac{-\pi}{4},\frac{7\pi}{4}\right],\ r\leq\rho(\theta)\right\},$$

where ρ is defined by:

$$\rho(\theta)=\begin{cases}\dfrac{a}{\cos(\theta)}\ \text{pour}\ \theta\in\left[\dfrac{-\pi}{4},\dfrac{\pi}{4}\right],\\ \dfrac{a}{\cos\left(\theta-\dfrac{\pi}{2}\right)}\ \text{pour}\ \theta\in\left[\dfrac{\pi}{4},\dfrac{3\pi}{4}\right],\\ \dfrac{a}{\cos(\theta-\pi)}\ \text{pour}\ \theta\in\left[\dfrac{3\pi}{4},\dfrac{5\pi}{4}\right],\\ \dfrac{a}{\cos\left(\theta-\dfrac{3\pi}{2}\right)}\ \text{pour}\ \theta\in\left[\dfrac{5\pi}{4},\dfrac{7\pi}{4}\right].\end{cases}$$

Let us consider the function $f:(r,\theta)\rightarrow r^n g(\theta)$. One a:

$$I=\int_\Omega f(r,\theta)\,dS=\int_0^{2\pi}\left(\int_0^{\rho(\theta)} f(r,\theta)\,r\,dr\right)d\theta.$$

Thus:

$$I=\int_0^{2\pi}\left(\int_0^{\rho(\theta)} r^{n+1}g(\theta)\,dr\right)d\theta=\frac{1}{n+2}\int_0^{2\pi} g(\theta)\left(\rho(\theta)\right)^{n+2}d\theta.$$

One a:

$$J=\int_0^{2\pi} g(\theta)\left(\rho(\theta)\right)^{n+2}d\theta=J_1+J_2+J_3+J_4,$$

with:

$$J_1=a^{n+2}\int_{\frac{-\pi}{4}}^{\frac{\pi}{4}}\frac{g(\theta)}{\cos(\theta)^{n+2}}d\theta,$$

$$J_2=a^{n+2}\int_{\frac{\pi}{4}}^{3\frac{\pi}{4}}\frac{g(\theta)}{\cos\left(\theta-\frac{\pi}{2}\right)^{n+2}}d\theta=a^{n+2}\int_{\frac{-\pi}{4}}^{\frac{\pi}{4}}\frac{g\left(\theta+\frac{\pi}{2}\right)}{\cos(\theta)^{n+2}}d\theta,$$

$$J_3=a^{n+2}\int_{\frac{3\pi}{4}}^{\frac{5\pi}{4}}\frac{g(\theta)}{\cos(\theta-\pi)^{n+2}}d\theta=a^{n+2}\int_{\frac{-\pi}{4}}^{\frac{\pi}{4}}\frac{g(\theta+\pi)}{\cos(\theta)^{n+2}}d\theta,$$

$$J_2=a^{n+2}\int_{\frac{5\pi}{4}}^{\frac{7\pi}{4}}\frac{g(\theta)}{\cos\left(\theta-\frac{3\pi}{2}\right)^{n+2}}d\theta=a^{n+2}\int_{\frac{-\pi}{4}}^{\frac{\pi}{4}}\frac{g\left(\theta+\frac{3\pi}{2}\right)}{\cos(\theta)^{n+2}}d\theta,$$

One thus has finally:

$$I=\frac{a^{n+2}}{n+2}\int_{\frac{-\pi}{4}}^{\frac{\pi}{4}}\frac{1}{\cos(\theta)^{n+2}}\left[g(\theta)+g\left(\theta+\frac{\pi}{2}\right)+g(\theta+\pi)+g\left(\theta+\frac{3\pi}{2}\right)\right]d\theta.$$

One notices that for $n=1$ and $g:\theta\rightarrow(\kappa-\cos(\theta))^2$. , one a:

$$I=\int_\Omega r(\kappa-\cos\theta)^2\,dS.$$

It is also noticed that:

$$(\kappa-\cos\theta)^2=\kappa^2+\frac{1}{2}-2\cos(\theta)+\frac{1}{2}\cos(2\theta).$$

One thus has in this case:

$$g(\theta)+g\left(\theta+\frac{\pi}{2}\right)+g(\theta+\pi)+g\left(\theta+\frac{3\pi}{2}\right)=4\kappa^2+2.$$

From where:

$$\int_\Omega r(\kappa-\cos\theta)^2\,dS=\frac{a^3}{3}(4\kappa^2+2)\int_{\frac{-\pi}{4}}^{\frac{\pi}{4}}\frac{1}{\cos(\theta)^3}d\theta.$$

And finally:

$$\|\boldsymbol{u}\|_{L^2}^2=\left(\frac{1+\nu}{E}\right)^2K_I^2a^3\frac{(2\kappa^2+1)}{3\pi}\int_{\frac{-\pi}{4}}^{\frac{\pi}{4}}\frac{1}{\cos(\theta)^3}d\theta.$$

That is to say:

$$\|\boldsymbol{u}\|_{L^2}=\frac{1+\nu}{E}K_Ia^{\frac{3}{2}}\sqrt{\frac{(2\kappa^2+1)}{3\pi}\int_{\frac{-\pi}{4}}^{\frac{\pi}{4}}\frac{1}{\cos(\theta)^3}d\theta}\approx 7{,}6057690825\times10^{-6}\,\mathrm{m}^2.$$

1.4.2 Calculation of the energy of the structure

The energy of the structure is defined by:

$$E^e=\frac{1}{2}\int_\Omega\boldsymbol{\sigma}:\boldsymbol{\varepsilon}\,dS.$$

Since $\nu=0$, one has $\boldsymbol{\varepsilon}=\frac{1}{E}\boldsymbol{\sigma}$. From where :

$$\boldsymbol{\sigma}:\boldsymbol{\varepsilon}=\frac{1}{E}\left(\sigma_{xx}^2+\sigma_{yy}^2+2\sigma_{xy}^2\right).$$

By using the form of the tensor of the constraints given previously and close developments, one obtains :

$$\boldsymbol{\sigma}:\boldsymbol{\varepsilon}=\frac{K_I^2}{E}\frac{1}{2\pi r}\left(2\cos\left(\frac{\theta}{2}\right)^2+2\cos\left(\frac{\theta}{2}\right)^2\sin\left(\frac{\theta}{2}\right)^2\right).$$

It is noticed that:

$$2\cos\left(\frac{\theta}{2}\right)^2=1+\cos\theta,$$

$$2\cos\left(\frac{\theta}{2}\right)^2\sin\left(\frac{\theta}{2}\right)^2=\frac{1}{2}\sin(\theta)^2=\frac{1}{4}(1-\cos(2\theta)).$$

One thus has:

$$\boldsymbol{\sigma}:\boldsymbol{\varepsilon}=\frac{K_I^2}{E}\frac{1}{2\pi r}\left(\frac{5}{4}+\cos(\theta)-\cos(2\theta)\right).$$

That is to say:

$$E^e=\frac{K_I^2}{E}\frac{1}{4\pi}\int_\Omega\frac{1}{r}\left(\frac{5}{4}+\cos(\theta)-\cos(2\theta)\right)dS.$$

One notices that for $n=-1$ and $g:\theta\rightarrow\frac{5}{4}+\cos(\theta)-\cos(2\theta)$. , one a:

$$I=\int_0^{\rho(\theta)}\frac{1}{r}\left(\frac{5}{4}+\cos(\theta)-\cos(2\theta)\right)d\theta.$$

One has in this case:

$$g(\theta)+g\left(\theta+\frac{\pi}{2}\right)+g(\theta+\pi)+g\left(\theta+\frac{3\pi}{2}\right)=5.$$

From where:

$$\int_\Omega\frac{1}{r}\left(\frac{5}{4}+\cos(\theta)-\cos(2\theta)\right)dS=5a\int_{\frac{-\pi}{4}}^{\frac{\pi}{4}}\frac{1}{\cos(\theta)}d\theta=5a\left(\ln(3)+2\sqrt{2}\right).$$

And finally:

$$E^e=\frac{K_I^2}{E}\frac{5a}{4\pi}\left(\ln(3)+2\sqrt{2}\right)\approx 3{,}50687407712\times10^{-6}\ \mathrm{J}\times\mathrm{m}^{-1}.$$

1.5 Bibliographical references

[1] GENIAUT S., MASSIN P.: eXtended Finite Method Element, Handbook of reference of *Code_Aster*, [R7.02.12]

[2] Rice, J.R. (1968), “with path independent integral and the approximate analysis of strain concentration by notches and aces”, *Newspaper of Applied Mechanics* **35**: 379-386

[3] Satzi, Belytschko: Year extended Finite Element Method with Higher-Order Elements for Curved Aces

[4] LABORDE P., APPLE TREE J., FOX Y., SALAUN Mr., “High-order extended finite element method for cracked domains”, International Newspaper for Numerical Methods in Engineering, vl.
64, pp. 354-381, 2005

2 Modeling A

In this modeling D_PLAN, the plate is fissured on a half-length. The crack is described by method XFEM. The crack is enriched geometrically, on a ray $R_{ENRI}=0,1$.

elements are linear of type TRIA3.

2.1 Characteristics of the grid

The unit square is with a grid regularly [Figure 2.1-1]. To build the grid, one is based on a regular squaring 100×100 .

MANY NODES: 10201

MANY MESHS: 20400
TRIA3: 20000

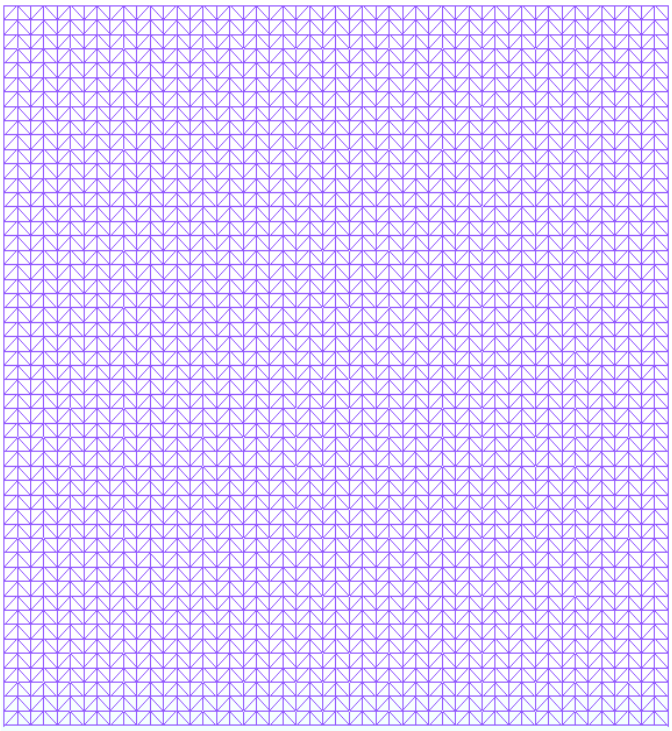

Figure 2.1-1: Grid with element-triangles

2.2 Sizes tested and results

2.2.1 Sizes tested:

For this horizontal crack, one tests the value of the stress intensity factors K_I and K_{II} as well as the value of the rate of refund of energy G data by CALC_G.

For the method $G-thêta$ (order CALC_G), one selected the following crown of field theta:

$R_{inf}=0,1\,a$ and $R_{\sup}=0,3\,a$ where a is the length of the crack.

In addition, one tests the field of displacement calculated by Code_Aster. Instead of carrying out a local test on some meshs by TEST_RESU, one tests the field of displacement on a large number of meshs. An arbitrary zone of test was delimited in the field [Figure 2.2.1-1].

In practice, one compares: $\left\|U^{calc}-U^{ana}\right\|_{L_2}<tolerance\times\left\|U^{ana}\right\|_{L_2}$.

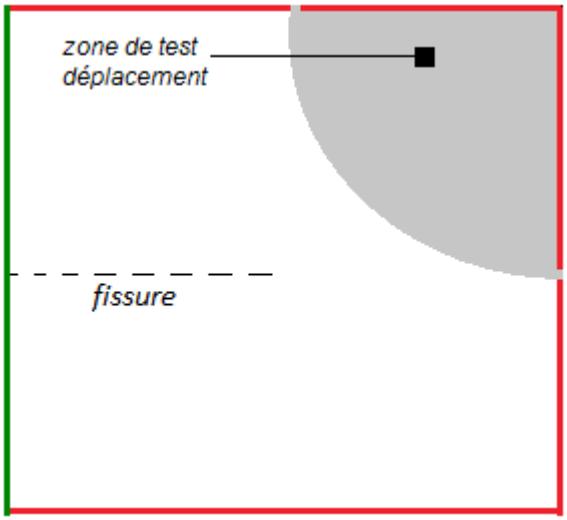

Figure 2.2.1-1: definition of GROUP_MA of test

One tests finally the energy of the structure the standard L^2 displacement.dans all the field.

2.2.2 Results:

Test of the stress intensity factors:

Identification	Reference	Tolerance
CALC_G		
K1	1,00	1,0%
K2	0,00	1,0%
G	$1.0\ 10^{-5}$	1,0%

Test of the norme_L2 of the error on the field of displacement: $\left\|U^{calc}-U^{ana}\right\|_{L_2}<tolerance\times\left\|U^{ana}\right\|_{L_2}$

Identification	Reference	Tolerance
POST_ELEM		
NORMALIZES	0,00	0,1%

Test of the energy of the structure:

Identification	Reference	Tolerance
POST_ERREUR		
REFERENCE	$3.50687407712\ 10^{-6}$	0,1%

Test of the standard L^2 déplacement.dans all the field :

Identification	Reference	Tolerance
POST_ERREUR		
REFERENCE	7.6057690825 10^{-6}	0,1%

2.3 Complementary results:

On [Figure 2.3-1], the field of displacement is represented with amplification of the jump of displacement to the interface. It is noted that the crack opens rigorously in $mode\,I$, as expected.

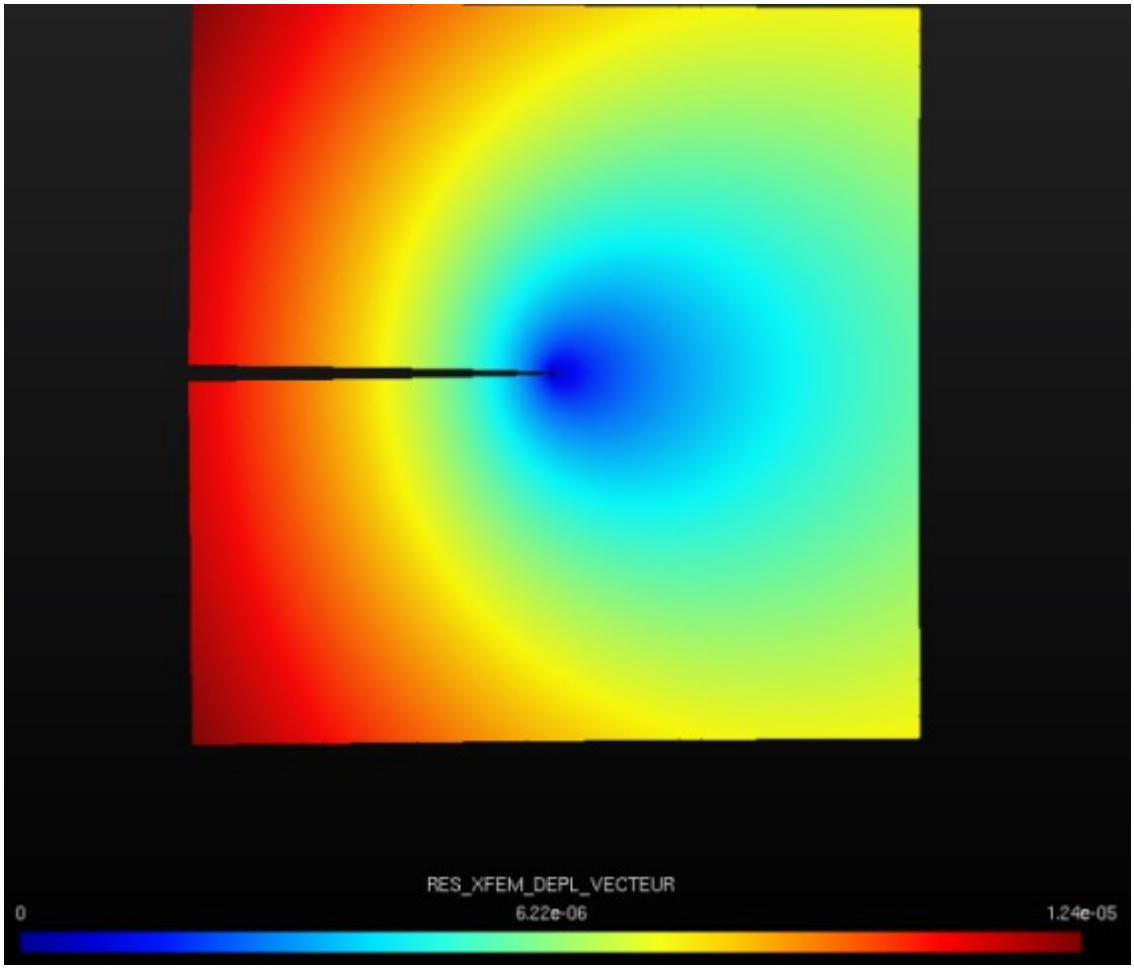

Figure 2.3-1: Field of displacement (with offset)

3 Modeling B

Modeling D_PLAN, with method XFEM to represent the crack. Quadratic elements TRIA6.

3.1 Characteristics of the grid

The unit square is with a grid regularly [Figure 2.1-1]. One preserves the refinement of preceding modeling.

MANY NODES: 40401

MANY MESHS: 20400
TRIA6: 20000

3.2 Sizes tested and results

One tests the same sizes as in modeling A, except for the energy of the structure and the standard L^2 déplacement.dans all the field.

Test of the stress intensity factors:

Identification	Reference	Tolerance
CALC_G		
K1	1,00	1,0%
K2	0,00	1,0%
G	$1.0\ 10^{-5}$	1,0%

4 Modeling C

Modeling D_PLAN, with method XFEM to represent the crack. Quadratic elements TRIA3.

4.1 Characteristics of the grid

The unit square is with a grid regularly [Figure 2.1-1]. One preserves the refinement of preceding modelings.

MANY NODES: 10201

MANY MESHS: 20400
TRIA3: 20000

4.2 Sizes tested and results

The same sizes are tested that in modeling B. One checks the stress intensity factors and the field of displacement on part of the field compared to the analytical values.

Let us note that for the definition of the zone of test, for a variable slope, one generalizes the approach of modeling A. According to the slope of the crack, one tests the corner of the field opposed to the crack (see [Figure 4.2-1] and [Figure 4.2-2]).

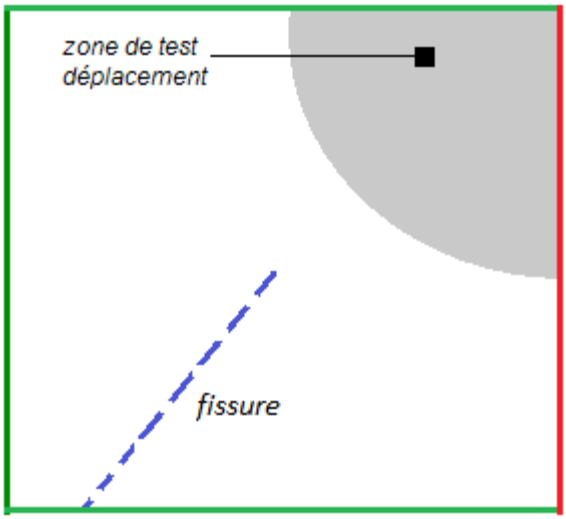

Figure 4.2-1: Definition of GROUP_MA of test

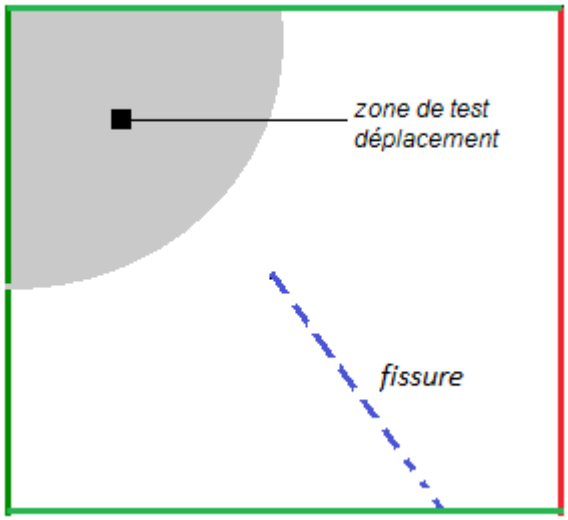

Figure 4.2-2: Definition of GROUP_MA of test

Test of the stress intensity factors:

Identification	Reference	Tolerance
CALC_G		
K1	1,00	1,0%
K2	0,00	1,0%
G	$1.0\ 10^{-5}$	1,0%

4.3 Complementary results

Ci below, one represents the field of displacement (with offset) for a variable slope of the crack.

5 Modeling D

Modeling C_PLAN, with method XFEM to represent the crack. Linear elements TRIA3.

5.1 Characteristics of the grid

The grid is identical to that of modeling A.

5.2 Sizes tested and results

One tests the same sizes as in modeling A.

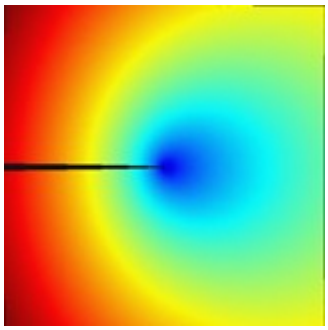
alpha=0°

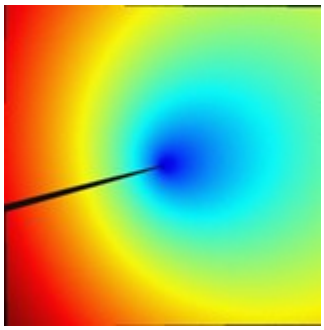
alpha=15°

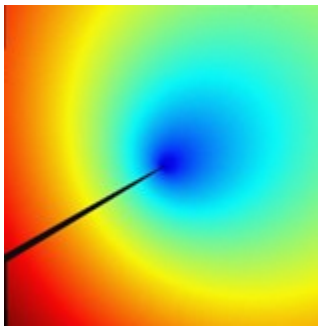
alpha=30°

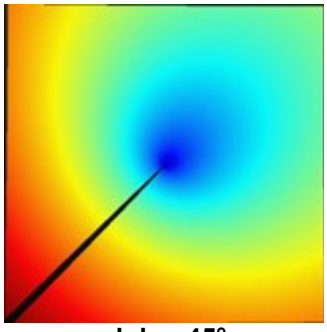
alpha=45°

Test of the stress intensity factors:

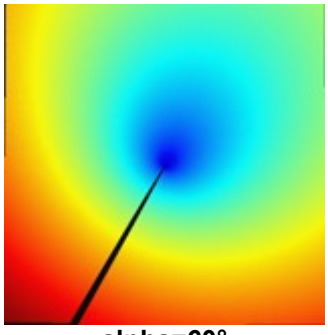
alpha=60°

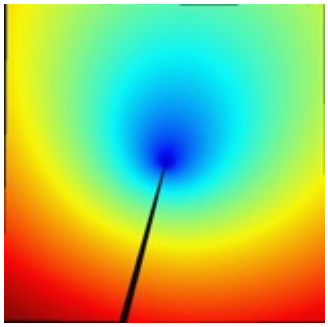
alpha=75°

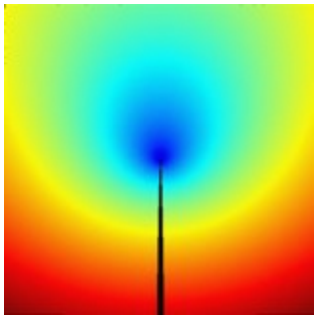
alpha=90°

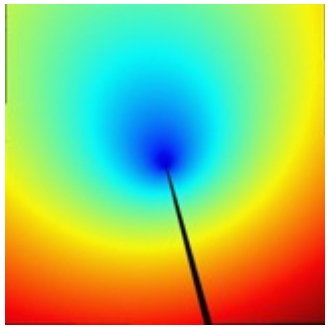
alpha=105°

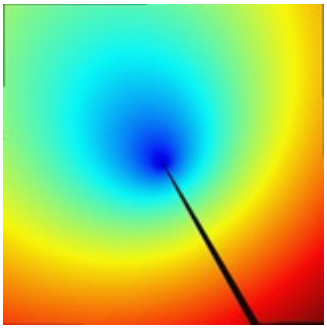
alpha=120°

Identification	Reference	Tolerance
CALC_G		
K1	1,00	1,0%
K2	0,00	1,0%

G	1.0 10^{-5}	1,0%

Test of the standard $L2$ error on the field of displacement:

Identification	Reference	Tolerance
POST_ELEM		
NORMALIZES	0,00	0,1%

Test of the energy of the structure:

Identification	Reference	Tolerance
POST_ERREUR		
REFERENCE	3.50687407712 10^{-6}	0,1%

Test of the standard L^2 déplacement.dans all the field :

Identification	Reference	Tolerance
POST_ERREUR		
REFERENCE	7.6057690825 10^{-6}	0,1%

6 Summary of the results

Modelings A, B, C and D show that method XFEM makes it possible to find the asymptotic field of the theory for a crack opening in mode I. It is noted that the field of displacement is accurately represented since, in particular, one finds the analytical values of the stress intensity factors.

In the paragraph [17], one restored the evolution of the field of displacements according to the angle of inclination, on a great angular beach. One diewatch as well as the field calculated displacement remains invariant in the local reference frame related to the crack: the asymptotic field “follows” the movement of the crack, in accordance with the theory. Consequently, the geometry of the field in the reference frame of the crack, the regularity and the “directionnality” of the grid, do not affect the precision of calculations of the CAS-test, with linear elements.

Moreover, one does not note the appearance of a zone of transition between the conditions from limits from Dirichlet and Neumann. For example in modeling C, the test on the standard $L2$ error in displacement, is carried out on the corner undergoing at the same time a loading of Neumann and a condition of
Dirichlet. The displacement calculated by Aster “sticks” to the analytical solution. Would it as have to be made sure as the same applies to stress field? Developments in the code_Aster should set up a calculation of the standard in energy to confirm these observations.

However, there exist 2 limitations with the validation presented above:

- On the one hand, the slope “ad infinitum” of the crack is not possible in our model. In modeling C, the angle of inclination is understood enters $-135°$ and $135°$ because of the condition limits of Dirichlet on one of the edges of the field. Being given the symmetry of the problem, to continue this study on the rest of the trigonometrical circle appears not relevant.
- In addition, modeling B shows that a validation is possible with quadratic elements. However, one indicates a significant degradation of conditioning.